Using c-fos immunohistochemistry to monitor pattern separation in the dentate gyrus.

Thomas Sollie
S3030814
06/07/2020
Supervisors: Youri Bolsius, Pim Heckman, Robbert Havekes

Abstract

In order to distinguish highly similar memories, an information process called pattern separation is needed. Here, overlapping sets of information are actively pulled apart. The dentate gyrus (DG) in the hippocampus has been implicated by fMRI and ECG studies in performing this function. It achieves PS via sparse baseline activity, high firing specificity and two processes called rate- and global remapping of cell ensembles. To this day, involvement has never been shown on a molecular level. Immediate early genes (IEGs) were used in this article to monitor neuronal activity in the DG following an object location memory task, or a behavioural test that elicited PS. In an immunohistochemical cell count of IEG positive cells, no overall increase of DG activity was found following active PS. Either PS is facilitated without overall activity increase, or the IEG method is insufficient to monitor it. Indeed, some articles report that c-fos positivity does not strongly correlate with neuronal firing, but rather represents performant path to DG input. Furthermore, one characteristic of PS is repeated reconsolidation of similar memories. With regards to this, zif268 reveals itself as a better candidate for IEG studies in the DG. Finally, whereas IEGs are insufficient to monitor rate remapping, they provides opportunities to study global remapping. While the method has obvious limitations, it has benefits over single cell recordings and whole brain scans.

Introduction

Throughout evolution, the hippocampus has become adapt at manipulating data. In the brains of humans and other vertebrates, efficient networks exist in order to process sets of information from environmental stimuli. Two of these processes are pattern completion (PC) and pattern separation (PS) (see Figure 1) (Hainmueller & Bartos, 2020; Yassa & Stark, 2011). The former allows for incomplete sets of information to be completed into the full reference memory. The latter concerns itself with two

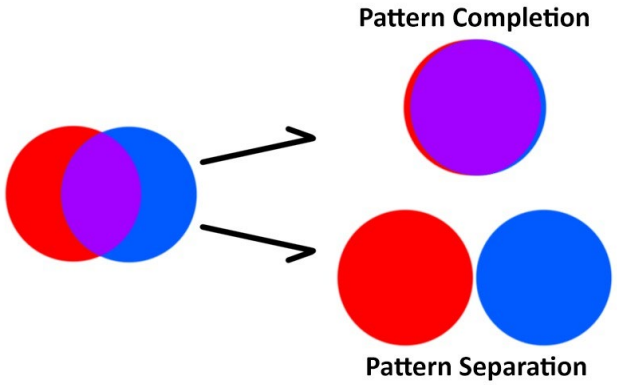

Figure 1 | A visualisation of PC and PS. The red and blue colours represent two sets of information. For a hippocampus specific example, one set can be visual stimuli, and the other a reference memory. Purple represents an overlap in information between both sets.

overlapping sets of information, allowing for similar sets to be recognised as two separate entities. In daily life, PS helps to distinguish a new situation to readily existing similar memories. For instance, when parking your car at the same parking lot, it is important to remember where you placed it today, versus where it was parked yesterday. A lack or failing of the process can lead to memory interference (Colgin et al., 2008), and an inability to distinguish similar experiences (Hainmueller & Bartos, 2020).

Extensive literature implicates the CA3 of the hippocampus (HPC) in recalling memories, and deems it adapt at performing PC (Nakazawa, 2017; Neunuebel & Knierim, 2014; Rolls, 2013; Yassa & Stark, 2011). The area consists of so called recurrent collaterals, or networks of neurons that can repeatedly activate each other until a local stability has been reached. This way, a full memory is recalled from only a fraction of input. However, such a network is unable to actively separate overlapping data sets. For PS to occur, a filter upstream of the CA3 is necessary. Indeed, the dentate gyrus (DG) is an upstream constituent of the CA3: information enters the HPC via the entorhinal cortex (EC), and either directly flows to the CA3 via the performant path (PP), or is processed by the DG before arriving at the CA3 (Amaral et al., 2007). Information flows directionally through the HPC, via the previously mentioned path, called the tri-synaptic loop. The DG is parallel to this loop, and can process

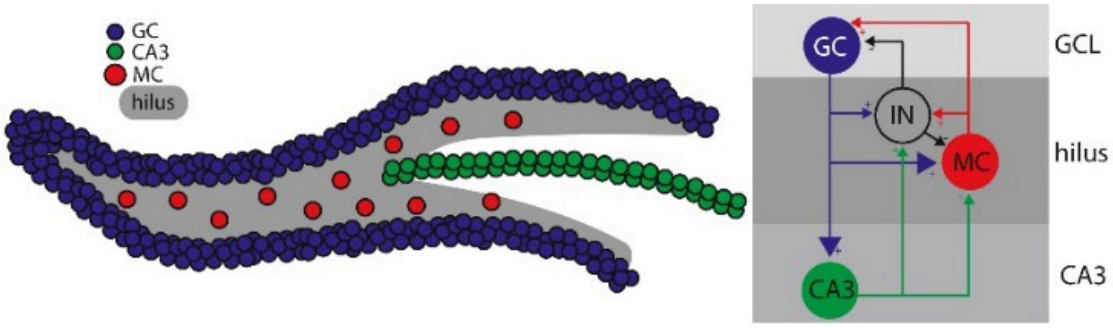

Figure 2 | *Adapted from Goodsmith et al., 2017.* Morphological (left) and cellular (right) mark-up of the DG. The DG wraps around the pCA3. Information enters from the PP into the GCs. Here, multiple feedback loops with MCs and other interneurons located in the hilus exist until a desired computation has been reached. The information is then sent from GCs to pyramidal CA3 cells.

incoming information differently. Therefore, it is stipulated that the DG functions as such a filter, and can effectively perform PS (GoodSmith et al., 2017, 2019; Hainmueller & Bartos, 2018, 2020; Neunuebel & Knierim, 2014; Yassa & Stark, 2011). Then, two sets consisting of new sensory information and a reference memory enter the DG simultaneously. The output is two separated sets of information, represented by two distinct ensembles of neurons.

Electrophysiological studies and computational models show the DG is able to achieve this via multiple different means (Hainmueller & Bartos, 2020; Schmidt et al., 2012). These means are not mutually exclusive, but are interconnected and work in tandem. First, a high abundance of granular cells (GCs) are present in the region (Amaral et al., 2007). Relatively few PP input enters this abundance of GCs, while each GC fires upon only a handful of CA3 pyramidal cells, meaning high specificity. This allows for respectively information divergence followed by information convergence, during which PS is likely to take place (Chavlis et al., 2017; J. K. Leutgeb et al., 2007). Under baseline conditions, the DG is sparsely active, and normally only shows low frequency firing (Hainmueller & Bartos, 2020). This way, GCs predominantly activate interneurons such as mossy cells (MCs) (see Figure 2). GCs and these interneurons repeatedly activate via feedback loops until a stable configuration of GCs has been reached (Hainmueller & Bartos, 2018). Then, this configuration of GCs fire in high frequency bursts upon CA3 pyramidal cells, passing on their information.

The second means for performing PS consists of remapping (S. Leutgeb et al., 2005; Santoro, 2013; Schmidt et al., 2012). This represents dynamically changing the neuronal representation of an environment. Due to the computation the DG performs, new and unique ensembles of cells are recruited within the CA3. These ensembles are non-overlapping in their information. Two types of remapping exist: rate remapping, represented by changes in cell firing rates; and global remapping, where an ensemble of neurons restructures (see Figure 3) (Colgin et al., 2008). In the former, within the DG the same cells are active for both sets of information, but certain cells will gradually start to represent one set more than the other (Santoro, 2013). The changes in rate encoding are then decoded when information reaches the CA3. Indeed, as previously mentioned, firing rate and magnitude of GCs are important for determining what cells in the CA3 are recruited. In global remapping, information within the DG is pulled apart and is gradually represented by different, orthogonal ensembles of cells. Then, due to sparse activity and a low contact probability of GCs onto pyramidal cells, unique ensembles within the CA3 are recruited (Santoro, 2013).

Part of the function the DG performs is that it has been implied in consolidating context to memories (Hainmueller & Bartos, 2020; Schmidt et al., 2012). Indeed, after blocking GC output, the direct PP to CA3 connection is sufficient to retrieve already established memories of CFC (Kitamura et al., 2015; Nakashiba et al., 2012), unless recall requires distinction between similar contexts (Bernier et al., 2017). As expected, ablation of GCs before CFC memory acquisition results in impaired storage of the similar contexts, and ablates task performance. Furthermore, the DG and PS can be implicated in reconsolidation of an already existing memory (Hainmueller & Bartos, 2020; J. L. C. Lee, 2010; Miranda & Bekinschtein, 2018). A readily existing memory is then put into a labile state. Here, new information in the form of context can be added to a memory, i.e. remembering where at the very familiar parking lot you parked your car today. As such, the DG is able to add context to memories, or highlight details in new memories (J. L. C. Lee, 2008, 2010). In order to achieve this, new information must be compared to a readily existing memory, after which integration of the new information takes place into the memory

trace. Here, PS could take place to facilitate the information integration.

Taken together, the DG performs a function of PS, and likely does so upon the CA3. It shows sparse firing, and lies parallel to the tri-synaptic loop. Therefore, it is likely to assume that the DG would only activate when needed, such as when performing a PS function. As such, an increase in overall DG activity is expected when actively performing PS.

Involvement of the DG in behavioural tasks calling upon PS has already been shown in both fMRI and ECG studies in both rodents and humans (Bakker et al., 2008; Lacy et al., 2011; J. K. Leutgeb et al., 2007; Treves et al., 2008). Indeed, activity in the region is seen when performing such a task. However, thus far it has not been shown on a molecular level that the DG is active during PS. One way to achieve this is to monitor cell activity in the DG via the use of immediate early gene (IEG) transcription. For example, the IEG c-fos can be used here as a marker for neuronal activity (Bernstein et al., 2019; Douglas et al., 1988; Guzowski et al., 1999; Hainmueller & Bartos, 2020). Whenever a neuron fires, protein levels of this transcription factor rapidly rise and remain elevated for several hours. Downstream are multiple growth and survival factors such as BDNF to increase cell proliferation, and plasticity between activated cells. Via histochemical analysis of c-fos positivity in cells within the subregions of the dorsal HPC, activity of these regions can be shown. By giving mice behavioural tasks requiring PS, overall activity of cells in the DG and other hippocampal regions can be compared.

The aim of the current study is to use a spatial memory task to illicit active PS in rodents, and to monitor the activity of the DG at a molecular level using c-fos. With that, more cell activation is expected in the DG following active PS.

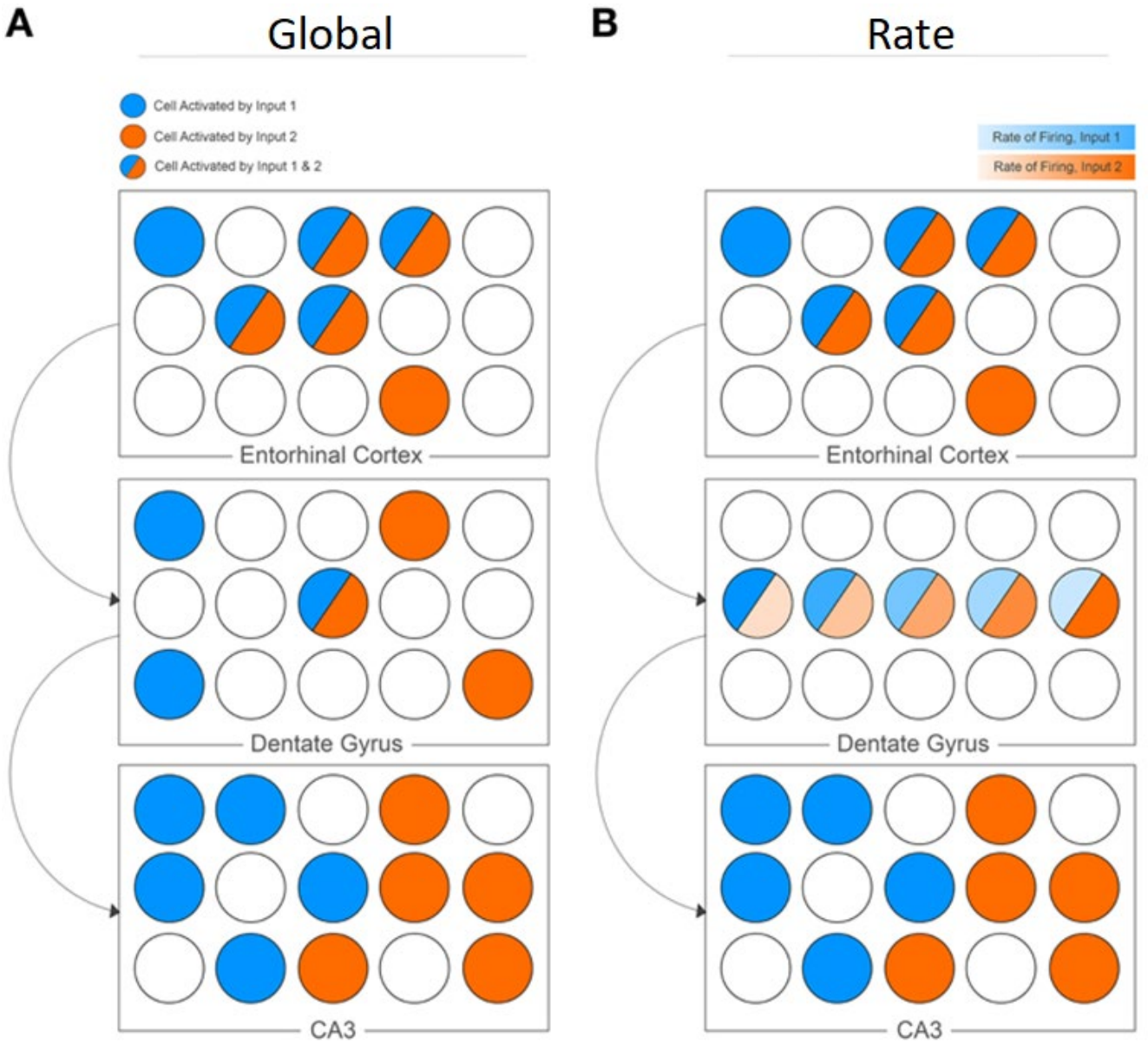

Figure 3 | *Adapted from Santoro, 2013.* The two types of remapping that constitute PS. (**A)** In global remapping, overlapping sets of information are gradually represented by orthogonal ensembles of cells before arriving in the CA3. (**B**) Rate remapping constitutes gradual changes in firing rates of neurons, until one of both sets of information is represented more than the other.

Methods

Animal care and housing

A total of 18 male C57BL/6J mice were randomly distributed among three experimental groups: OLM, OPS and control (n=6). The animals were ordered from Charles River and were aged 42-48 days at arrival. After arrival, the animals were dual housed for two weeks and then moved into single housing. A standard 12 hr light and dark cycle was maintained (lights on at 10:00 to 22:00), and the room was kept at a steady temperature of 22°. Food and water were available ad libitum. One day after movement to single housing, habituation followed for four consecutive days. This consisted of three days of human handling for 3 min daily, and one day four habituation to the testing arena for 10 min. All of the habituation and behavioural testing were performed at the start of the light phase.

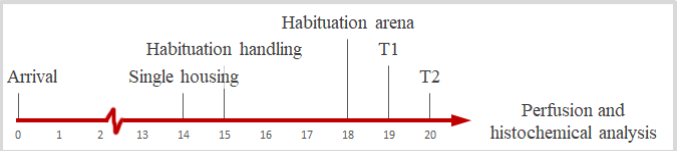

Figure 4 | Timeline of behavioural experiment in days. 60m after T2, animals were perfused for further histochemical analysis.

Behavioural testing

The experimental groups were tested via one of two similar location memory tests: the object location memory (OLM), and object pattern separation (OPS) task (see Figure 5). All animals were tested in two consecutive trials each lasting 10 min. In the training trial (T1), objects were placed perpendicular to each other. After 24h followed the testing trial (T2). Here, one of the objects was moved to a new location of 1-5, where 1 is the starting position, and each step represents a dislocation of 3.75 cm. These locations were previously determined in own research, as described by van Goethem et al. (2018). For OPS position 3, and for OLM position 5 was determined. Objects in the control group were not moved in T2, but rather stayed perpendicular as presented previously in T1. Due to the innate curiosity of rodents, they will spend more time exploring the moved object. This exploration time is then measure. The distance of movement for the object is smaller for OPS; it was previously determined as the minimum distance an object had to be moved in order for the mice to notice. Thus in context of an identical environment, a small adjustment was made to the new sensory information, requiring PS (van Goethem et al., 2018; van Hagen et al., 2015). This test is an adaption from the OLM task, and as such formation of memory relies on the HPC (Hainmueller & Bartos, 2020). As such, the DG is necessary for retrieval of said memories, and is thus required for spatial memory pattern separation (Gilbert et al., 2001; I. Lee & Solivan, 2010).

The arena used for this task has the following dimensions: a width of 30 cm, a length of 40 cm and a height of 50 cm. At either side across the width of the arena cues were present in the form of a striped and a checkerboard pattern. For the objects, one out of four possible sets of household objects was used, randomly distributed among experimental groups. The same set of objects was used per animal for both trials. Determination and direction of movement of the objects in T2 was done following a randomisation scheme, and was consistent among experimental groups. Objects were placed 7.5 cm from the side walls, and at position 5, objects are still 5 cm away from the length walls.

Footage was captured and subsequently analysed using manual scoring. Exploration time per object, and total exploration time were measured. From this, a discrimination index (d2) was calculated as: (time_replaced – time_old) / (time_replaced + time_old), to control for total exploration.

During both trials, total exploration time of both objects combined was calculated as e1 and e2, for T1 and T2 respectively.

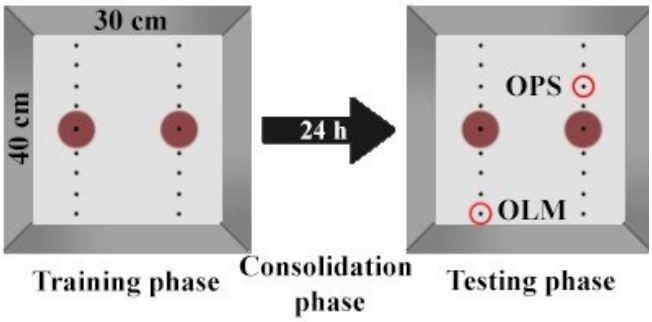

Figure 5 | The two trials of the OLM and OPS behavioural tasks. The dark red dots represent the objects. Each object can be moved to either the 3rd position (for OPS) or the 5th position (OLM), as depicted by the red circles.

Immunohistochemistry

Perfusion of animals was performed 60 min after T2 using 4% PFA. Brains were then washed in PBS and stored in PBS + Azide. To freeze the brains, samples were put in a 30% sucrose solution overnight. Brains were frozen in liquid nitrogen before being stored at -80°. Slices of the HPC were cut at 20um using a cryostat, and were stored in PBS + Azide in 4° cold storage. For analysis, only slices from the dorsal HPC were used.

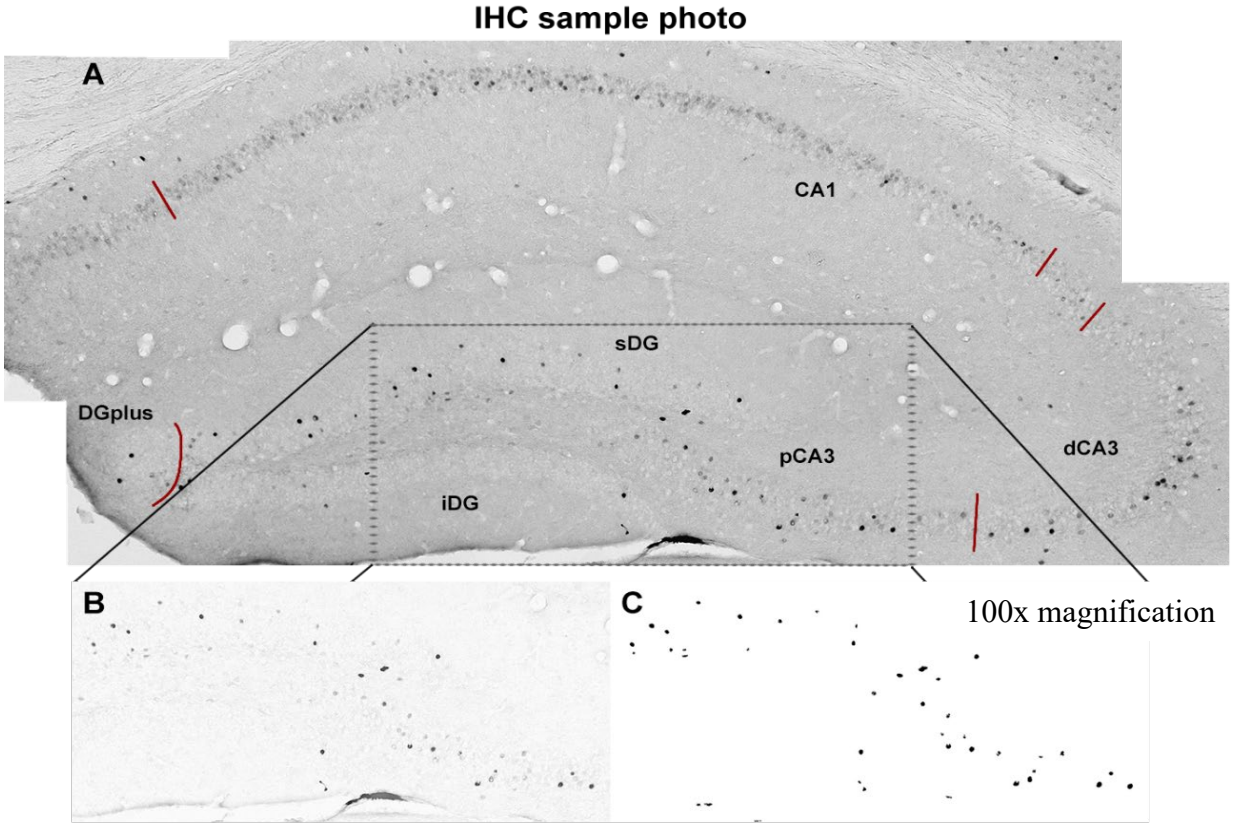

Figure 6 | A photo of the entire HPC from a random sample. The red lines represent the determination of regions. For the outlined box, the image processing and overlay are shown. (**A**) The merged picture without processing. (**B**) The same picture with the background subtracted and added contrast. (**C**) A *middle* overlay mask, made for the source photo.

To visualise c-fos, an immunohistochemistry (IHC) DAB staining was performed. Slices were selected for their quality. These were treated with hydrogen peroxide (0.3%) to halt activity of peroxidases in the tissue. Slices were then permeabilised in 0.3% Triton-X and simultaneously a pre-blocking treatment was done with normal goat serum for 1 hr. For the primary antibody, a 1:2000 dilution was used (Abcam #ab208942, RRID: AB_2747772), and slices were incubated for 72 hr in 4° cold storage on a shaker. Then, slices were incubated for 2 hr in the secondary antibody, which consisted of Biotinylated goat-anti-mouse IgG at 1:400 dilution. The AB complex (Vectastain PK-6100 standard) for visualisation was prepared 30 min in advance at a dilution of 1:500, and treatment was done for 2 hr. The final DAB incubation time was determined at 11:30 min with the use of two test cups. All washing steps for the IHC protocol were done with PBS on a shaker.

Mounting of slides was done with a 1% gelatine solution in PBS. A total of 6-8 slices were mounted per slide. Slides were then dried overnight and dehydrated in an ethanol/xylol series. Finally, they were covered with DPX and cover glass.

C-fos positivity cell counting

From each sample's slide, three brain slices were selected for the structural quality of their HPC. From these slices, photos were taken of the entire HPC bilaterally. This was done using a Leika microscope at a magnification of 100x. Multiple photos of one HPC were stitched together using photoshop.

These merged photos were then processed using ImageJ (see Figure 6; for more on ImageJ, see supplementary information). For each photo, the same series of processing steps were applied using automated scripts. This was done to aid in cell counting in a similar fashion for all sample photos. First, a background subtraction was done (Figure 6B) to equalise brightness across pictures. Second, an overlay mask (Figure 6C) was created to determine cell positivity. This overlay only colours groups of pixels above a certain black value, size and circularity. Three separate overlays were made, with different settings for a threshold determining which cells are deemed positive. These overlays are called *low, middle* and *high.* Settings for the original overlay (*middle*) were determined manually from a few random sample pictures as reference. From this, the other two overlays were created with a higher and lower threshold.

The number of positive cells were counted manually to increase accuracy of the measurements. Cells were counted for each region of the HPC separately (Figure 6A). Different regions of the HPC can be discerned. For this experiment, the following were chosen: superior DG (sDG), inferior DG (iDG), DGplus, proximal CA3 (pCA3), distal CA3 (dCA3),

and CA1. For each sample and region, averages were taken from the six photos of that sample (three slices bilaterally). Only cells in the granular cell layers were counted.

DGplus represents the very tip of the DG where both blades meet. This area was measured separately as it is unclear which of the two blades the positive cells belong to. In calculations involving the entire DG, this measurement was included in the summation. The CA3 is separated into the dCA3 and pCA3. This was done via a measurement of the total length of the CA3, and taking the first 40% to be proximal (as described by GoodSmith et al., 2019; H. Lee et al., 2015). Measurement for the CA3 starts at the granular cell layer between the end of the two DG blades. The region ends at the CA2 (excluded in analyses), after which the CA1 starts. From this final region, the very end was excluded.

The dichotomy of the CA3 was chosen as the pCA3 has been implicated in PS (GoodSmith et al., 2017; H. Lee et al., 2015). From the pyramidal cells of the CA3, back projections exist upon interneurons within the DG (Figure 2, left). This way, the pCA3 is likely to benefit PS.

All slices were taken from the dorsal HPC. Along its axis, this part is especially involved in spatial memory tasks (Ferbinteanu & Mcdonald, 2000; I. Lee & Kesner, 2003; Pothuizen et al., 2004). Expression of multiple different IEGs has been shown to increase following tasks that test this memory (Guzowski et al., 1999, 2001). It has repeatedly been used to study PS in the DG (I. Lee & Kesner, 2004; Satvat et al., 2011; Schmidt et al., 2012).

Sample 10 was removed from all analyses due to problems during perfusion and IHC. Furthermore, from the IHC a separate analysis was done using a reduced dataset. All samples with poor image quality were removed from this analysis. Poor quality consisted of crystallisation or problems during perfusion. These samples consisted of: 1 (all regions except the DG), 4, 8, 10, 11, 12 and 14.

Statistics

All statistics were performed in SPSS v25.

From the behavioural tests, the d2 scores were compared. A one-way ANOVA was performed to check for differences between all groups. One-sample t-tests were performed to test significance of experimental groups against zero. Independent sample t-tests were performed to check whether groups differed significantly from each other. Inherent to the OLM and OPS behavioural tasks is that the animal will explore the moved object more than the unmoved object. A negative d2 value is thus not ever expected for these groups. As such, a one-tailed t-test could also be performed.

For HPC, a Welch's t-test was performed to check for significant differences between experimental groups. A one-way ANOVA was done to check for any difference between all groups.

As a final analysis, a possible correlation between the behavioural tests and the IHC was analysed. The d2 scores of individual mice were coupled to their IHC count. A linear regression analysis was done to check for significance.

All graphs present were created using GraphPad Prism 8. The regression analysis was also performed using this program.

Results

Behavioural tasks

The graph for behavioural testing is shown in Figure 7. For the d2 scores, performing a one-way Welch ANOVA across al experimental groups revealed significant differences ($p = 0.038$). Indeed, in a one-sample t-test OLM statistically differed from chance ($p = 0.020$), and in an independent sample t-test against control (unequal variances, $p = 0.021$). Although OPS showed a clear trend, no positive results for this group were found in either the one-sample t-test ($p = 0.123$) or the t-test against control (unequal variances, $p = 0.167$). When performing a one-tailed, one sample t-test for OPS, results were just short of significance ($p = 0.061$).

Neither the e1 nor e2 scores differed between groups. A one-way Welch ANOVA for either

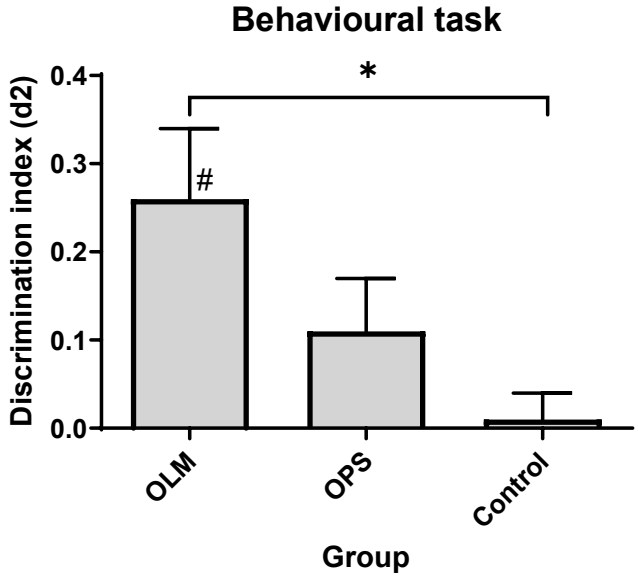

Figure 7 | The d2 score for all three experimental groups. OLM shows a significant difference from zero (one-sample t-test, $^{\#}p < 0.05$). The group also has a higher d2 score than control (t-test, $^{*}p < 0.05$).

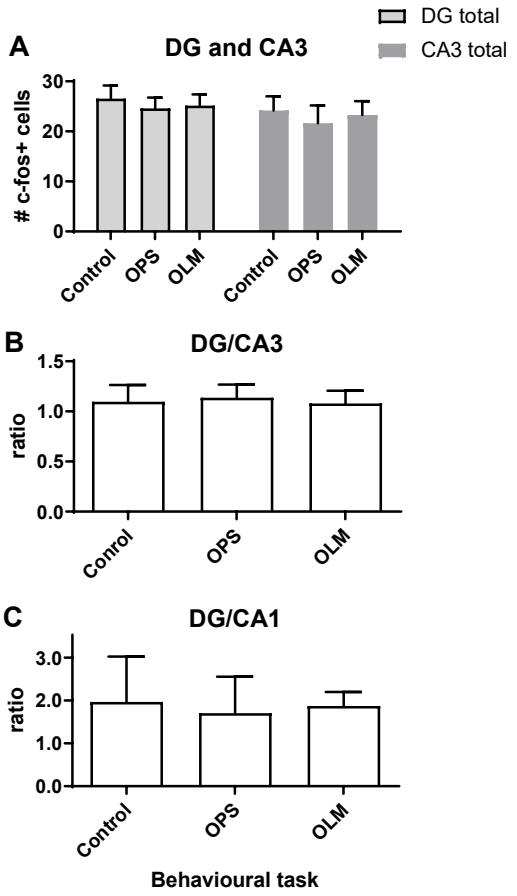

Figure 8 | IHC results of middle overlay. (**A**) Total cell counts for the entire DG and CA3 for all three groups. (**B**) The ratio of DG divided by CA3 cell counts. (**C**) The ratio of DG divided by CA3 cell counts.

revealed no statistical variance ($p = 0.26$ and $p = 0.53$ respectively). This means the total exploration times in T1 or T2 were the same for all groups, as expected.

Immunohistochemistry

Analysis of the cell counts did not reach statistical significance. None of the regions between groups showed differences in their mean from either t-tests or ANOVAs. This was true for all three overlays.

Figure 8 shows graphs for the *middle* overlay only. Here, 8A shows total cell counts for the DG, and for the CA3. No differences were found between groups for either of these summations. The second graph shows the ratio of DG to CA3 positive cells. As the DG is expected to be involved in PS, whereas the CA3 has been implicated in PC, the ratio was expected to be substantially higher for the OPS group than for the OLM group. Again, this is not reflected in the results. Finally 8C shows the ratio of DG activation versus that of the CA1. Here, an attempt is made to normalise activation of the DG, as the CA1 is not necessarily involved in either PS or PC, and is likely to have a similar level of activation in both (Guzowski et al., 2004; Hunsaker & Kesner, 2008).

A second analysis was performed using only a subset of the entire dataset. Here, all images with low quality were excluded. However, again no significant results were found in statistical testing.

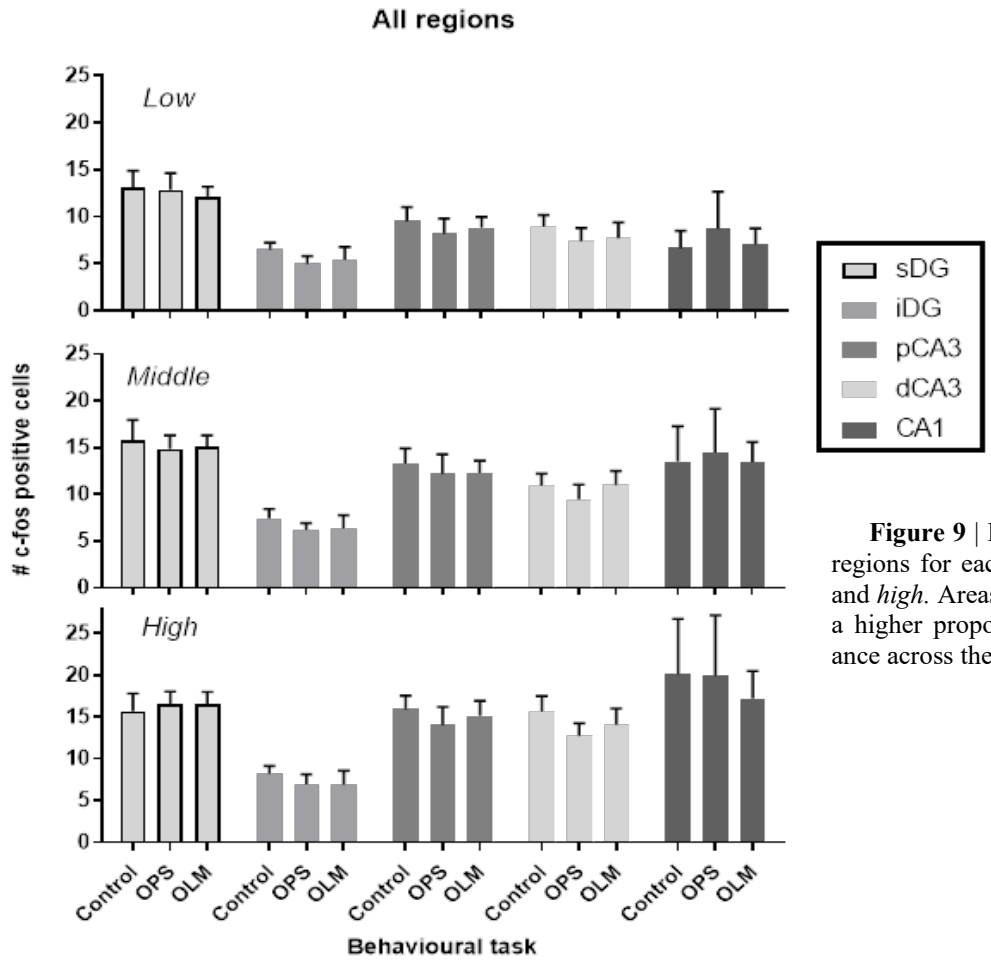

Figure 9 | Raw cell counts from all counted regions for each overlay threshold *low, middle* and *high.* Areas further away from the DG show a higher proportional increase, and more variance across the thresholds.

When comparing the three overlay thresholds, it is interesting to notice that especially the CA1 and to a lesser extend CA3 show a larger proportional increase (see Figure 9 *low* and *high*). Furthermore, the overlays show more variance as the threshold was set higher. Especially the high overlay has large variances for the CA1. Both of these observations are consistent with the IHC photos, where these regions show many cells with more light grey tints, whereas the DG shows clearly defined black dots (Figure 6).

Correlation d2 and IHC

An inquiry for a possible correlation between the behavioural tests and the cell count was performed. This was done via a regression analysis. Here, the d2 values of samples from either the OLM or OPS group were plotted against their respective counts for individual regions. Animals that perform better on the behavioural task, might then also show more neuron positivity.

For the OPS, no significant results were found. The graph for the DG and CA3 regions is shown in Figure 10A.

A positive correlation was found for the CA3 within the OLM group (Figure 10B). A higher d2 score here is indicative of more cell positivity (*low* overlay: $R^2 = 0.87$, $p = 0.020$). Interesting to note here is that from the individual CA3 regions in the *low* count, the pCA3 showed no correlation ($R^2 = 0.54$, $p = 0.156$), while the dCA3 did ($R^2 = 0.80$, $p = 0.039$). Further, the ratio DG/CA3 showed a result in line with the CA3 finding, which is expected (*low* overlay: $R^2 = 0.91$, $p = 0.013$).

Finally, an analysis was done adding cell counts from both the OPS and OLM groups together to increase the sample size. However, when comparing this group to the control, again nothing of interest was found.

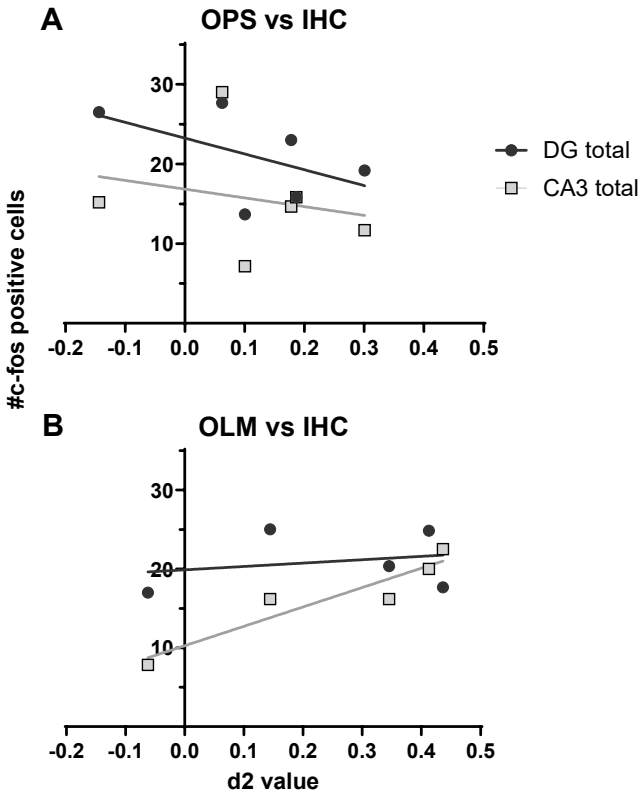

Figure 10 | Regression analysis of d2 values plotted against the respective IHC counts for the *low* overlay. (**A**) No significant result found for a regression of the OPS samples. (**B**) Within the OLM samples, a higher d2 score is indicative of more CA3 cell positivity ($R^2 = 0.87$, $p = 0.020$).

Discussion

The results from this article do not reveal an increase in DG activity. Either PS is facilitated without increasing overall activity, or the IEG method used in this article is insufficient to monitor it. The results can be explained in a variety of ways. Here, multiple are mentioned, and possible opportunities for follow-up studies using IEGs are given.

DAB time, sample size and image quality

In less sparse firing of neurons in regions like the CA1, many partly positive cells were present in IHC pictures. It is probable that longer DAB incubation times would increase contrast in these regions of the HPC. However, DAB time is unlikely to play a role in overall results: neurons in the DG showed clear activation with little ambiguity. This is visible in the comparison of overlays, where *high* shows little more positive cells in this region compared to *low* (Figure 9).

Due to low tissue quality, some samples were likely not a good indicator for their relative group. This was mostly due to crystallisation of water, problems during perfusion and handling slices during cutting and IHC. Thus, a reduced analysis of cell counts was done with these samples excluded. As a result of this, sample size per group was severely reduced (n = 3 for OLM and OPS). It is possible that such a reduces sample size negatively influenced statistical analysis of both the cell counts and correlations.

Overall, the question remains whether a sample size of six animals is high enough to accurately perform a regression analysis. A general rule of thump states a minimum of ten samples is needed (Hair et al., 2014).

Finally, the d2 score of the OPS group was not able to reach statistical significance from either control or zero. Indeed, the original experiment required an

n=12 for the behavioural tests, which was not realised. Therefore, it remains unproven that these animals actually were able to notice the dislocation of objects in this task. However, it is unlikely this influences results of the IHC as the d2 scores show a clear trend, even with n=6. In line with the reduced analysis from the IHC, a follow-up study could benefit from a larger sample size.

IEGs as a marker for neuronal activity

One of the primary roles of IEGs is to induce plasticity changes, and thereby consolidate a memory. However, as the DG is not required for retrieval, presumably the DG does not store a memory itself, but rather helps encode it in the CA3, and via systems consolidation in other parts of the brain. It is assumable then that plastic changes within the DG are not linked directly to a memory, but rather to the computations the DG performs. Specifically, plastic changes would then program the DG to perform future computations more accurately, or to differently influence CA3 wiring. Transcription of IEGs is underlying these plasticity changes. The question then remains in what way IHC cell positivity actually reflects cell activity in the DG. When using IEG techniques, it is important to realise what is being measured.

Pyramidal cells are only activated by GCs once they receive high burst activity (Henze et al., 2002; Mori et al., 2004). In contrast, interneurons show a low threshold for firing, indicating that low frequency firing of GCs predominantly targets interneurons. These interneurons in their turn inhibit GC firing (Chavlis et al., 2017). This way, a stable set of GCs is reached, and following high burst firing, information progresses to the CA3 (Hainmueller & Bartos, 2018). Nuances in firing rate are thus important for DG functioning. However, IEG imaging techniques might not be able to detect this as they cannot detect rate remapping, and are not fully correlated with the total amount of neuronal firing (Schmidt et al., 2012).

In line with this, some articles report that c-fos positivity in GCs does not strongly correlate with neuronal firing, but rather indicate an NMDA receptor activation (Kim et al., 2018; Labiner et al., 1993). Indeed, activation of this receptor in GCs results in increased synaptic plasticity (Hainmueller & Bartos, 2020). The widespread presence of GABAergic and other receptor type interneurons that make up DG feedback loops thus fail to provide information via IEG expression of GCs. For example, MC to GC firing undergoes LTP, and is integral to DG functioning, but is independent of the NMDA receptor (Hashimotodani et al., 2017). Firing of an achieved stable GC ensemble thus might not be represented by transcription of the c-fos gene. Overall, c-fos positivity is more indicative of DG input, as PP firing onto GCs reliably results in activation of the NMDAR, and expression of the IEG (Hainmueller & Bartos, 2020; Labiner et al., 1993). Then, c-fos would not be an accurate marker when looking at overall activity.

Zif268, reconsolidation and LTP

When using IEG imaging techniques in the DG, c-fos might not be the best candidate. Instead, zif268 presents itself as a better option. This regulatory gene is involved in plasticity, and transcription has been implicated after neuronal activity in the DG (Schmidt et al., 2012). Within the DG, it is deemed a valid indicator of cell activation, as it can reliably replicate findings of single cell firing, and other electrophysiological studies (Jung & McNaughton, 1993; J. K. Leutgeb et al., 2007). The gene is activated by the MEK/ERK pathway, with CREB being a transcription factor (Davis et al., 2003). Levels of this factor are in itself increased following neuronal activation (Moore et al., 1996), as Ca^{2+} influx results in CREB phosphorylation (Kornhauser et al., 2002). Upregulation of the IEG is seen after stimulation of many types of receptors, including glutamatergic, adrenergic, dopaminergic, and opiate receptors (Beckmann & Wilce, 1997; Hughes & Dragunow, 1995). Furthermore, it has been used to prove GC global remapping following in similar context behavioural test trials (Satvat et al., 2011). Indeed, it has been shown to be involved in spatial learning and CFC memory formation (Davis et al., 2003). Finally, zif268 KO mice show impaired proliferation and morphological defects in adult newborn GCs (Veyrac et al., 2013). These subtypes of GCs are in particular involved in PS, and storage of memories for CFC (Hainmueller & Bartos, 2020; Nakashiba et al., 2012). Without the gene, a severe reduction in responsiveness of these neurons is observed, and LTM of spatial learning fails (Veyrac et al., 2013).

As mentioned, a working theory of PS involves consolidating new context to existing memories. In order to achieve this, the memory would have to be put into a state of reconsolidation. This is relevant to the present study, as PS is performed in comparing new context to an already existing memory from T1; a form of reconsolidation thus is likely to take place. Zif268 as an IEG is especially involved in reconsolidation. An experiment by Bozon et al. (2003) showed this in the dorsal HPC following the object recognition task. Here, zif268 KO and WT mice were repeatedly exposed to an environment for 5 min periods. Then after either two or five days, in T2 one object was replaced, and exploration of both objects was measured. These mice, as well as WT, showed

no trouble retrieving memories. However, if anywhere between T1 and T2 the KO animals were briefly exposed to both the arena and objects of T1 (thus eliciting reconsolidation), they showed impairments of memory at the T2 retention test. This indicates a role of the gene especially in controlling plasticity during reconsolidation. Indeed, in a similar task, zig268 mutant mice show impaired LTM formation after normal, but not after extensive training trials; memories after bouts of reconsolidation are reliably impaired (Jones et al., 2001; J. L. C. Lee et al., 2004). After normal training trials with a full KO mouse model, consolidation is insufficient to form a memory, and mice show a deficit in memory when tested for either consolidation or reconsolidation (Besnard et al., 2013). With a one allele KO model, consolidation was sufficient, but still reconsolidation was impaired. Finally, repeats of the same spatial learning tasks reliably induce transcription of zif268 within the dorsal HPC (Guzowski et al., 2001).

In line with it's role in reconsolidation, the gene has been heavily implicated in playing a role in LTP and long-term memory formation. In the DG, LTP induction is correlated with zif268 upregulation (Abraham et al., 1993; Richardson et al., 1992). This is specific to LTP persistence, while initial magnitude does not contribute. Specifically, zif268 seems to stabilize long-lasting LTP, and thus is a major indicator for inducing lasting plasticity changes (Jones et al., 2001). LTP in its turn has been linked to PS. Induction of potentiation in MC to GC feedback loops helps DG output, and enhances PS (Hashimotodani et al., 2017). Furthermore, silencing of NMDA receptors significantly reduces GC plasticity, and these mice show impaired CFC performance (McHugh et al., 2007). More specifically, in GluN2A KO models, mice show impaired synaptic plasticity, and fail at a variety of spatial pattern separation tasks (Kannangara et al., 2014). With regards to LTP, c-fos paints a different picture. LTP induction in the PP does not reliably result in c-fos transcription in GCs (Douglas et al., 1988; Dragunow et al., 1989). Furthermore, transcription is not correlated with the amount of LTP (Dragunow et al., 1989). Indeed, induction of LTP in the DG shows little correlation with c-fos mRNA levels following a northern blot (Wisden et al., 1990).

Taken together, this data implicates a role of zif268 in all both consolidation and especially reconsolidation, and shows a better response to induction of LTP than c-fos. However, articles discussing either LTP or IEG transcription often exclusively focus on the DG, while looking past the CA3. As mentioned, the DG induces plasticity changes in this HPC area (Hainmueller & Bartos, 2020). It might do this as a function to induce plasticity changes at the level of pyramidal cells in the CA3, without necessarily resulting in changes within the DG itself. When using IEGs, behaviour of the CA3 is therefore important to incorporate into the results. Overall, the use of zif268 in monitoring CG activity in the DG seems better suited, especially for the experiment performed in this paper.

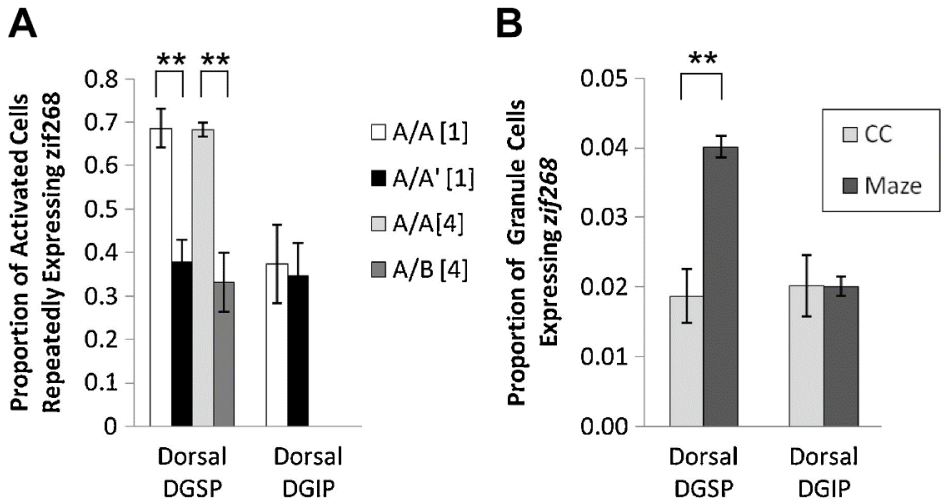

Figure 11 | *Adapted from Schmidt et al., 2012.* Similar and distinct environments both highly decrease DG activity overlap. (**A**) The proportion of cells that overlap in activation across two behavioural tasks (Marrone et al., 2011). A stark decrease in overlap is seen in the superior blade of the DG (DGSP) when using two distinct environments (A/B) but also in the same environment with an altered task demand (A/A'), when compared to exposure to the same environment twice (A/A). This is also true for the ventral DG (not shown), but not for the inferior blade (DGIP). (**B**) Exposure to a task substantially increases IEG positivity in the superior blade of the DG (DGSP) when compared to home cage control. This is true for the ventral DG (not shown), but not for the inferior blade (DGIP).

Using IEGs to determine GC remapping in the DG

As mentioned, remapping is the manner via which the DG facilitates PS. Were the DG to function exclusively via rate remapping, the lack of overall activated cells from IHC results in this article could be explained. However, extensive research from single cell recordings and IEG studies indicates global remapping to take place (J. K. Leutgeb et al., 2007; Nakazawa, 2017; Satvat et al., 2011; Schmidt et al., 2012). Indeed, both types of remapping are underlying PS (Hainmueller & Bartos, 2020; Schmidt et al., 2012). As mentioned, rate remapping cannot be visualised via IEGs. Global remapping can be, however, and one method that is explained below is particularly interesting to explore this feature. As an advantage, it presents a picture for the entire DG and HPC, where single cell recordings are highly limited in scale. If the IEG visualisation used in this paper is insufficient to monitor changes in overall activity, the global remapping method still provides interesting opportunities.

The method is an *in-situ* hybridization technique that is used to timestamp IEG cell positivity (Schmidt et al., 2012). As first described by Guzowski et al. (1999), this technique tracks IEG transcription responses to two distinct time points. For *Arc* and *zif268*, within minutes of neuronal activity, RNA accumulates in the nucleus. This RNA then disappears, and reappears 30 min after neuronal activity as an accumulation in the cytoplasm outside of the nucleus. This allows performing two consecutive behavioural tasks with the same animal, and determining IEG activity separately for both.

Using this method, one can elucidate behaviour of global remapping of GCs in the DG. Remapping is described here by the difference in overlap in IEG positivity between both epochs of behavioural tests. When testing the same rat for two different navigational strategies within a plus maze (Figure 11A, A/A'), significantly less GCs show repeated activation compared to testing the same strategy (1st A/A), indicating remapping of GCs (Satvat et al., 2011). Indeed, if a rat does the same task twice in the same environment (2nd A/A), 70% of cells overlap in activity (Marrone et al., 2011), which is substantially higher when compared to distinct environments (A/B). Still, this overlap is above 90% for pyramidal cells (Guzowski et al., 1999), from which the authors conclude that remapping is still present if tested in the same environment, but on separate occasions.

Small changes in environment, strategy, or even solely temporal, reveal the high tendency of remapping for GCs. Regardless of the degree of contextual differences, remapping of the DG is substantial. This could be why for the IHC in this paper, a similar level of DG activity was seen in all groups, as DG activity in the form of remapping was true for all groups. Even the control group would then show DG activity, due to the time elapsed between T1 and T2, giving new temporal context.

Reducing overlap of CA3 pyramidal cell activity

A recent theory on how the DG facilitates PS has gained popularity. The theory stems from observations that CA3 activity patterns differ more between similar contexts than those of the DG (Hainmueller & Bartos, 2018; Senzai & Buzsáki, 2017). Furthermore, in a study using the previously mentioned overlapping IEG method, animals that were better at discriminating two similar environments were those that showed a higher IEG overlap in ensembles of the DG (Marrone et al., 2011).

The theory states that the two sets of information enter the DG, after which only the overlapping part is sent forward to the CA3. Simultaneously, the same sets are projected to the CA3. From the DG via inhibitory interneurons, pyramidal cells are silenced, and only parts of the ensembles in the CA3 that are not overlapping remain activated. Indeed, KO mouse models of this interneuron show an increase in overlap of CA3 ensembles (Ruediger et al., 2011). Thus for similar environments, ensembles in the DG are fused, only mapping that which is consistent across similar contexts, but purposefully excluding information about details.

If this theory were true, in the method used in this experiment, fused information would have been present the DG comparing the environment seen in T2 to the environment in the reference memory of T1. Then, this ensemble would be similar for all behavioural groups, as all animals are exposed twice to similar environments. Now it is probable that the IEG activity method would be insufficiently sensitive to detect differences in overall cell activity between the groups.

In line with this, exposure to a behavioural task such as the y-maze substantially increases IEG positivity in the superior blade of the DG (Figure 11B) and the entire HPC (Miyashita et al., 2009). Even exposure to the control environment of the experiment in this paper could thus lead to a considerable amount of DG cell positivity. For a follow-up study, a home cage control should be added to see if the behavioural task in itself elicits an increase in IEG cell positivity.

Blades of the DG & CA3 workings

The superior blade of the DG shows substantially more activation than the inferior blade (Figure 9). This is not surprising as Amaral et al. (2007) report a 1.5 fold higher number of GCs in the superior blade of rats compared to its counterpart. Use of other IEGs like *Arc* and *zif268* show a similar ratio of activation for both blades as seen in the results of this experiment (Schmidt et al., 2012). Besides structural changes, the blades appear to function differently too. Figure 11 shows a difference between blades when testing for overlap of IEG activation between two consecutive behavioural tasks. This means that remapping of GCs after being exposed to a behavioural task affects the superior, but not the inferior blade. The morphology of the DG is different than other hippocampal areas. This probably aids in its functioning. When examining the full workings of the DG, it is important to recognise these details.

A positive correlation was found between OLM task performance and cell activity in the CA3 (Figure 9B). Specifically, the distal CA3 showed a correlation, while the proximate end did not. Indeed, the dorsal CA3 appears to play a role in spatial location memory (Gilbert & Brushfield, 2009). Specific lesions of this HPC region resulted in impaired performance for object-place paired behavioural tasks (Gilbert & Kesner, 2003). As the (distal) CA3 has been shown to perform pattern completion, retrieval of an OLM memory here could be indicative of this process. Then, more activity in the dCA3 would result in more pattern completion, and better recall of the memory.

Much is yet unclear about the exact role of the DG in PS. Ambiguity remains around the function of the different cell types, blades and cell ages, and the exact way the DG adds might add context to readily existing memories. The use of IEG has limitations, and results should be approached with caution. Still, these visualisation methods provide opportunities that are unreachable by single cell recordings or whole brain scans.

References

Abraham, W. C., Mason, S. E., Demmer, J., Williams, J. M., Richardson, C. L., Tate, W. P., Lawlor, P. A., & Dragunow, M. (1993). Correlations between immediate early gene induction and the persistence of long-term potentiation. *Neuroscience*, *56*(3), 717–727. https://doi.org/10.1016/0306-4522(93)90369-Q

Amaral, D. G., Scharfman, H. E., & Lavenex, P. (2007). *The dentate gyrus: fundamental neuroanatomical organization (dentate gyrus for dummies)*.

Bakker, A., Kirwan, C. B., Miller, M., & Stark, C. E. L. (2008). Pattern separation in the human hippocampal CA3 and dentate gyrus. *Science*, *319*(5870), 1640–1642. https://doi.org/10.1126/science.1152882

Beckmann, A. M., & Wilce, P. A. (1997). Egr transcription factors in the nervous system. In *Neurochemistry International* (Vol. 31, Issue 4, pp. 477–510). Pergamon. https://doi.org/10.1016/S0197-0186(96)00136-2

Bernier, B. E., Lacagnina, A. F., Ayoub, A., Shue, F., Zemelman, B. V., Krasne, F. B., & Drew, M. R. (2017). Dentate gyrus contributes to retrieval as well as encoding: Evidence from context fear conditioning, recall, and extinction. *Journal of Neuroscience*, *37*(26), 6359–6371. https://doi.org/10.1523/JNEUROSCI.3029-16.2017

Bernstein, H. L., Lu, Y. L., Botterill, J. J., & Scharfman, H. E. (2019). Novelty and novel objects increase c-fos immunoreactivity in mossy cells in the mouse dentate gyrus. *Neural Plasticity*, *2019*. https://doi.org/10.1155/2019/1815371

Besnard, A., Caboche, J., & Laroche, S. (2013). Recall and Reconsolidation of Contextual Fear Memory: Differential Control by ERK and Zif268 Expression Dosage. *PLoS ONE*, *8*(8). https://doi.org/10.1371/journal.pone.0072006

Bozon, B., Davis, S., & Laroche, S. (2003). A requirement for the immediate early gene zif268 in reconsolidation of recognition memory after retrieval. *Neuron*, *40*(4), 695–701. https://doi.org/10.1016/S0896-6273(03)00674-3

Chavlis, S., Petrantonakis, P. C., & Poirazi, P. (2017). Dendrites of dentate gyrus granule cells contribute to pattern separation by controlling sparsity. *Hippocampus*, *27*(1), 89–110. https://doi.org/10.1002/hipo.22675

Colgin, L. L., Moser, E. I., & Moser, M. B. (2008). Understanding memory through hippocampal remapping. In *Trends in Neurosciences* (Vol. 31, Issue 9, pp. 469–477). Elsevier Current Trends. https://doi.org/10.1016/j.tins.2008.06.008

Davis, S., Bozon, B., & Laroche, S. (2003). How necessary is the activation of the immediate early gene zif 268 in synaptic plasticity and learning? *Behavioural Brain Research*, *142*(1–2), 17–30. https://doi.org/10.1016/S0166-4328(02)00421-7

Douglas, R. M., Dragunow, M., & Robertson, H. A. (1988). High-frequency discharge of dentate granule cells, but not long-term potentiation, induces c-fos protein. *Molecular Brain Research*, *4*(3), 259–262. https://doi.org/10.1016/0169-328X(88)90033-2

Dragunow, M., Abraham, W. C., Goulding, M., Mason, S. E., Robertson, H. A., & Faull, R. L. M. (1989). Long-term potentiation and the induction of c-fos mRNA and proteins in the dentate gyrus of unanesthetized rats. *Neuroscience Letters*, *101*(3), 274–280. https://doi.org/10.1016/0304-3940(89)90545-4

Ferbinteanu, J., & Mcdonald, R. J. (2000). Dorsal and ventral hippocampus: Same or different? In *Psychobiology* (Vol. 28, Issue 3).

Gilbert, P. E., & Brushfield, A. M. (2009). The role of the CA3 hippocampal subregion in spatial memory: A process oriented behavioral assessment. *Progress in Neuro-Psychopharmacology and Biological Psychiatry*, *33*(5), 774–781.

https://doi.org/10.1016/j.pnpbp.2009.03.037
Gilbert, P. E., & Kesner, R. P. (2003). Localization of function within the dorsal hippocampus: the role of the CA3 subregion in paired-associate learning. *Behavioral Neuroscience*, *117*(6), 1385.
Gilbert, P. E., Kesner, R. P., & Lee, I. (2001). Dissociating hippocampal subregions: A double dissociation between dentate gyrus and CA1. *Hippocampus*, *11*(6), 626–636. https://doi.org/10.1002/hipo.1077
GoodSmith, D., Chen, X., Wang, C., Kim, S. H., Song, H., Burgalossi, A., Christian, K. M., & Knierim, J. J. (2017). Spatial Representations of Granule Cells and Mossy Cells of the Dentate Gyrus. *Neuron*, *93*(3), 677-690.e5. https://doi.org/10.1016/j.neuron.2016.12.026
GoodSmith, D., Lee, H., Neunuebel, J. P., Song, H., & Knierim, J. J. (2019). Dentate Gyrus Mossy Cells Share a Role in Pattern Separation with Dentate Granule Cells and Proximal CA3 Pyramidal Cells. *The Journal of Neuroscience : The Official Journal of the Society for Neuroscience*, *39*(48), 9570–9584. https://doi.org/10.1523/JNEUROSCI.0940-19.2019
Guzowski, J. F., Knierim, J. J., & Moser, E. I. (2004). Ensemble Dynamics of Hippocampal Regions CA3 and CA1. *Neuron*, *44*(Figure 1), 581–584. http://www.ncbi.nlm.nih.gov/pubmed/15541306
Guzowski, J. F., McNaughton, B. L., Barnes, C. A., & Worley, P. F. (1999). Environment-specific expression of the immediate-early gene Arc in hippocampal neuronal ensembles. *Nature Neuroscience*, *2*(12), 1120–1124. https://doi.org/10.1038/16046
Guzowski, J. F., Setlow, B., Wagner, E. K., & McGaugh, J. L. (2001). Experience-dependent gene expression in the rat hippocampus after spatial learning: A comparison of the immediate-early genes Arc, c-fos, and zif268. *Journal of Neuroscience*, *21*(14), 5089–5098. https://doi.org/10.1523/JNEUROSCI.21-14-05089.2001
Hainmueller, T., & Bartos, M. (2018). Parallel emergence of stable and dynamic memory engrams in the hippocampus. *Nature*, *558*(7709), 292–296. https://doi.org/10.1038/s41586-018-0191-2
Hainmueller, T., & Bartos, M. (2020). Dentate gyrus circuits for encoding, retrieval and discrimination of episodic memories. In *Nature Reviews Neuroscience* (Vol. 21, Issue 3, pp. 153–168). Nature Research. https://doi.org/10.1038/s41583-019-0260-z
Hair, J. F., Black, W. C., Babin, B. J., & Anderson, R. E. (2014). *Multivariate Data Analysis* (7th editio). Pearson Education Limited.
Hashimotodani, Y., Nasrallah, K., Jensen, K. R., Chávez, A. E., Carrera, D., & Castillo, P. E. (2017). LTP at Hilar Mossy Cell-Dentate Granule Cell Synapses Modulates Dentate Gyrus Output by Increasing Excitation/Inhibition Balance. *Neuron*, *95*(4), 928-943.e3. https://doi.org/10.1016/j.neuron.2017.07.028
Henze, D. A., Wittner, L., & Buzsáki, G. (2002). Single granule cells reliably discharge targets in the hippocampal CA3 network in vivo. *Nature Neuroscience*, *5*(8), 790–795. https://doi.org/10.1038/nn887
Hughes, P., & Dragunow, M. (1995). Induction of immediate-early genes and the control of neurotransmitter-regulated gene expression within the nervous system. *Pharmacological Reviews*, *47*(1).
Hunsaker, M. R., & Kesner, R. P. (2008). Evaluating the differential roles of the dorsal dentate gyrus, dorsal CA3, and dorsal CA1 during a temporal ordering for spatial locations task. *Hippocampus*, *18*(9), 955–964. https://doi.org/10.1002/hipo.20455
Jones, M. W., Errington, M. L., French, P. J., Fine, A., Bliss, T. V. P., Garel, S., Charnay, P., Bozon, B., Laroche, S., & Davis, S. (2001). A requirement for the immediate early gene Zif268 in the expression of late LTP and long-term memories. *Nature Neuroscience*, *4*(3), 289–296. https://doi.org/10.1038/85138
Jung, M. W., & McNaughton, B. L. (1993). Spatial selectivity of unit activity in the hippocampal granular layer. *Hippocampus*, *3*(2), 165–182. https://doi.org/10.1002/hipo.450030209
Kannangara, T. S., Eadie, B. D., Bostrom, C. A., Morch, K., Brocardo, P. S., & Christie, B. R. (2014). GluN2A−/− Mice Lack Bidirectional Synaptic Plasticity in the Dentate Gyrus and Perform Poorly on Spatial Pattern Separation Tasks. *Cerebral Cortex*, *25*(8), 2102–2113. https://doi.org/10.1093/cercor/bhu017
Kim, S., Kim, Y., Lee, S. H., & Ho, W. K. (2018). Dendritic spikes in hippocampal granule cells are necessary for long-term potentiation at the perforant path synapse. *ELife*, *7*. https://doi.org/10.7554/eLife.35269
Kitamura, T., Sun, C., Martin, J., Kitch, L. J., Schnitzer, M. J., & Tonegawa, S. (2015). Entorhinal Cortical Ocean Cells Encode Specific Contexts and Drive Context-Specific Fear Memory. *Neuron*, *87*(6), 1317–1331. https://doi.org/10.1016/j.neuron.2015.08.036
Kornhauser, J. M., Cowan, C. W., Shaywitz, A. J., Dolmetsch, R. E., Griffith, E. C., Hu, L. S., Haddad, C., Xia, Z., & Greenberg, M. E. (2002). CREB transcriptional activity in neurons is regulated by multiple, calcium-specific phosphorylation events. *Neuron*, *34*(2), 221–233. https://doi.org/10.1016/S0896-6273(02)00655-4
Labiner, D. M., Butler, L. S., Cao, Z., Hosford, D. A., Shin, C., & McNamara, J. O. (1993). Induction of c-fos mRNA by kindled seizures: Complex relationship with neuronal burst firing. *Journal of Neuroscience*, *13*(2), 744–751. https://doi.org/10.1523/jneurosci.13-02-00744.1993
Lacy, J. W., Yassa, M. A., Stark, S. M., Muftuler, L. T., & Stark, C. E. L. (2011). Distinct pattern separation related transfer functions in human CA3/dentate and CA1 revealed using highresolution fMRI and variable mnemonic similarity. *Learning and Memory*, *18*(1), 15–18. https://doi.org/10.1101/lm.1971111
Lee, H., Wang, C., Deshmukh, S. S., & Knierim, J. J. (2015). Neural Population Evidence of Functional Heterogeneity along the CA3 Transverse Axis: Pattern Completion versus Pattern Separation. *Neuron*, *87*(5), 1093–1105. https://doi.org/10.1016/j.neuron.2015.07.012
Lee, I., & Kesner, R. P. (2003). Time-dependent relationship between the dorsal hippocampus and the prefrontal cortex in spatial memory. *Journal of Neuroscience*, *23*(4), 1517–1523. https://doi.org/10.1523/jneurosci.23-04-01517.2003
Lee, I., & Kesner, R. P. (2004). Encoding versus retrieval of spatial memory: Double dissociation between the dentate gyrus and the perforant path inputs into CA3 in the dorsal hippocampus. *Hippocampus*, *14*(1), 66–76. https://doi.org/10.1002/hipo.10167
Lee, I., & Solivan, F. (2010). Dentate gyrus is necessary for disambiguating similar object-place representations. *Learning and Memory*, *17*(5), 252–258. https://doi.org/10.1101/lm.1678210
Lee, J. L. C. (2008). Memory reconsolidation mediates the strengthening of memories by additional learning. *Nature Neuroscience*, *11*(11), 1264–1266. https://doi.org/10.1038/nn.2205
Lee, J. L. C. (2010). Memory Reconsolidation Mediates the Updating of Hippocampal Memory Content. *Frontiers in Behavioral*

Neuroscience, *4*(NOV), 168. https://doi.org/10.3389/fnbeh.2010.00168
Lee, J. L. C., Everitt, B. J., & Thomas, K. L. (2004). Independent Cellular Processes for Hippocampal Memory Consolidation and Reconsolidation. *Science*, *304*(5672), 839–843. https://doi.org/10.1126/science.1095760
Leutgeb, J. K., Leutgeb, S., Moser, M. B., & Moser, E. I. (2007). Pattern separation in the dentate gyrus and CA3 of the hippocampus. *Science*, *315*(5814), 961–966. https://doi.org/10.1126/science.1135801
Leutgeb, S., Leutgeb, J. K., Barnes, C. A., Moser, E. I., McNaughton, B. L., & Moser, M. B. (2005). Independent codes for spatial and episodic memory in hippocampal neuronal ensembles. *Science*, *309*(5734), 619–623. https://doi.org/10.1126/science.1114037
Marrone, D. F., Adams, A. A., & Satvat, E. (2011). Increased pattern separation in the aged fascia dentata. *Neurobiology of Aging*, *32*(12), 2317.e23-2317.e32. https://doi.org/10.1016/j.neurobiolaging.2010.03.021
McHugh, T. J., Jones, M. W., Quinn, J. J., Balthasar, N., Coppari, R., Elmquist, J. K., Lowell, B. B., Fanselow, M. S., Wilson, M. A., & Tonegawa, S. (2007). Dentate gyrus NMDA receptors mediate rapid pattern separation in the hippocampal network. *Science*, *317*(5834), 94–99. https://doi.org/10.1126/science.1140263
Miranda, M., & Bekinschtein, P. (2018). Plasticity Mechanisms of Memory Consolidation and Reconsolidation in the Perirhinal Cortex. In *Neuroscience* (Vol. 370, pp. 46–61). Elsevier Ltd. https://doi.org/10.1016/j.neuroscience.2017.06.002
Miyashita, T., Kubik, S., Haghighi, N., Steward, O., & Guzowski, J. F. (2009). Rapid activation of plasticity-associated gene transcription in hippocampal neurons provides a mechanism for encoding of one-trial experience. *Journal of Neuroscience*, *29*(4), 898–906. https://doi.org/10.1523/JNEUROSCI.4588-08.2009
Moore, A. N., Neal Waxham, M., & Dash, P. K. (1996). Neuronal activity increases the phosphorylation of the transcription factor cAMP response element-binding protein (CREB) in rat hippocampus and cortex. *Journal of Biological Chemistry*, *271*(24), 14214–14220. https://doi.org/10.1074/jbc.271.24.14214
Morl, M., Abegg, M. H., Gähwiler, B. H., & Gerber, U. (2004). A frequency-dependent switch from inhibition to excitation in a hippocampal unitary circuit. *Nature*, *431*(7007), 453–456. https://doi.org/10.1038/nature02854
Nakashiba, T., Cushman, J. D., Pelkey, K. A., Renaudineau, S., Buhl, D. L., McHugh, T. J., Barrera, V. R., Chittajallu, R., Iwamoto, K. S., McBain, C. J., Fanselow, M. S., & Tonegawa, S. (2012). Young dentate granule cells mediate pattern separation, whereas old granule cells facilitate pattern completion. *Cell*, *149*(1), 188–201. https://doi.org/10.1016/j.cell.2012.01.046
Nakazawa, K. (2017). Dentate Mossy Cell and Pattern Separation. In *Neuron* (Vol. 93, Issue 3, pp. 465–467). Cell Press. https://doi.org/10.1016/j.neuron.2017.01.021
Neunuebel, J. P., & Knierim, J. J. (2014). CA3 retrieves coherent representations from degraded input: Direct evidence for CA3 pattern completion and dentate gyrus pattern separation. *Neuron*, *81*(2), 416–427. https://doi.org/10.1016/j.neuron.2013.11.017
Pothuizen, H. H. J., Zhang, W. N., Jongen-Rêlo, A. L., Feldon, J., & Yee, B. K. (2004). Dissociation of function between the dorsal and the ventral hippocampus in spatial learning abilities of the rat: A within-subject, within-task comparison of reference and working spatial memory. *European Journal of Neuroscience*, *19*(3), 705–712. https://doi.org/10.1111/j.0953-816X.2004.03170.x
Richardson, C. L., Tate, W. P., Mason, S. E., Lawlor, P. A., Dragunow, M., & Abraham, W. C. (1992). Correlation between the induction of an immediate early gene, zif/268, and long-term potentiation in the dentate gyrus. *Brain Research*, *580*(1–2), 147–154. https://doi.org/10.1016/0006-8993(92)90938-6
Rolls, E. T. (2013). The mechanisms for pattern completion and pattern separation in the hippocampus. In *Frontiers in Systems Neuroscience* (Vol. 7, Issue OCT, p. 74). Frontiers. https://doi.org/10.3389/fnsys.2013.00074
Ruediger, S., Vittori, C., Bednarek, E., Genoud, C., Strata, P., Sacchetti, B., & Caroni, P. (2011). Learning-related feedforward inhibitory connectivity growth required for memory precision. *Nature*, *473*(7348), 514–518. https://doi.org/10.1038/nature09946
Santoro, A. (2013). Reassessing pattern separation in the dentate gyrus. *Frontiers in Behavioral Neuroscience*, *JUL*. https://doi.org/10.3389/fnbeh.2013.00096
Satvat, E., Schmidt, B., Argraves, M., Marrone, D. F., & Markus, E. J. (2011). Changes in task demands alter the pattern of zif268 expression in the dentate gyrus. *Journal of Neuroscience*, *31*(19), 7163–7167. https://doi.org/10.1523/JNEUROSCI.0094-11.2011
Schmidt, B., Marrone, D. F., & Markus, E. J. (2012). Disambiguating the similar: The dentate gyrus and pattern separation. *Behavioural Brain Research*, *226*(1), 56–65. https://doi.org/10.1016/j.bbr.2011.08.039
Senzai, Y., & Buzsáki, G. (2017). Physiological Properties and Behavioral Correlates of Hippocampal Granule Cells and Mossy Cells. *Neuron*, *93*(3), 691-704.e5. https://doi.org/10.1016/j.neuron.2016.12.011
Treves, A., Tashiro, A., Witter, M. E., & Moser, E. I. (2008). What is the mammalian dentate gyrus good for? In *Neuroscience* (Vol. 154, Issue 4, pp. 1155–1172). Pergamon. https://doi.org/10.1016/j.neuroscience.2008.04.073
van Goethem, N. P., van Hagen, B. T. J., & Prickaerts, J. (2018). Assessing spatial pattern separation in rodents using the object pattern separation task. *Nature Protocols*, *13*(8), 1763–1792. https://doi.org/10.1038/s41596-018-0013-x
van Hagen, B. T. J., van Goethem, N. P., Lagatta, D. C., & Prickaerts, J. (2015). The object pattern separation (OPS) task: A behavioral paradigm derived from the object recognition task. *Behavioural Brain Research*, *285*, 44–52. https://doi.org/https://doi.org/10.1016/j.bbr.2014.10.041
Veyrac, A., Gros, A., Bruel-Jungerman, E., Rochefort, C., Kleine Borgmann, F. B., Jessberger, S., & Laroche, S. (2013). Zif268/egr1 gene controls the selection, maturation and functional integration of adult hippocampal newborn neurons by learning. *Proceedings of the National Academy of Sciences of the United States of America*, *110*(17), 7062–7067. https://doi.org/10.1073/pnas.1220558110
Wisden, W., Errington, M. L., Williams, S., Dunnett, S. B., Waters, C., Hitchcock, D., Evan, G., Bliss, T. V. P., & Hunt, S. P. (1990). Differential expression of immediate early genes in the hippocampus and spinal cord. *Neuron*, *4*(4), 603–614. https://doi.org/10.1016/0896-6273(90)90118-Y

Yassa, M. A., & Stark, C. E. L. (2011). Pattern separation in the hippocampus. In *Trends in Neurosciences* (Vol. 34, Issue 10, pp. 515–525). Elsevier Current Trends. https://doi.org/10.1016/j.tins.2011.06.006